Development of Porous Polymer Monolith by Photoinitiated Polymerization

Suzhu Yu, Feng Lin Ng, Khin Cho Cho Ma, Fern Lan Ng, Jianhong Zhao, Steven Kin Kong Tong

Singapore Institute of Manufacturing Technology, 71 Nanyang Drive, Singapore

Received 19 March 2010; accepted 12 August 2010
DOI 10.1002/app.33207
Published online 11 February 2011 in Wiley Online Library (wileyonlinelibrary.com).

ABSTRACT: Porous polymer monoliths have been successfully prepared by photoinitiated polymerization of butyl methacrylate (BMA) and ethylene glycol dimethacrylate (EDMA) monomers in porogenic solvent of methanol. Mercury intrusion porosimetry and scanning electron microscope are used to characterize the porous properties; nevertheless, the pore size obtained from both techniques is not comparable. The porous structure of the porous polymers is controlled by the phase separation during the polymerization and crosslinking. By varying the composition of the starting solution such as initiator fraction, BMA/EDMA ratio, porogen fraction, and UV intensity, porous polymers with median pore size from about 140 nm to 3 μm can be obtained, and the pore size distribution for majority of the porous polymers is also narrow. The results present a very positive prospect to microfluidic applications. © 2011 Wiley Periodicals, Inc. J Appl Polym Sci 120: 3190–3195, 2011

Key words: porous polymer; porous properties; photoinitiated polymerization; mercury porosimetry; microfluidics

INTRODUCTION

Porous polymers with interconnected pores have been widely used in many industries since a few decades ago. They can be used or act as support for ion-exchange resins, catalysts, adsorbents, chromatography, and so on.[1] The recently developed microfluidic technology has further enlarged the application areas of porous polymers. Microfluidics is a science to study and control of properties of fluids flowing in one or more channels with dimension less than 1 mm. Microfluidic devices have been developed for conducting, on a very small scale, a variety analytical and biochemical laboratory processes. By implementation of a flow restriction such as porous polymer in a microchannel network, the functions of the microfluidic devices are further enhanced to achieve the desired filtration, separation, detection, extraction, selective transport, and so on.

There are many ways to develop porous polymers.[2–4] Jong et al.[5] reported a replication method to produce porous polymer with tunable porosity on a silicon mold. The polymer was dissolved in a solvent and formed the polymer solution, which was cast on a microstructured mold, then the mold was immersed in another solvent, which is poor to the polymer, and the solvents exchange led to phase separation and left porous polymer with pore size up to several microns on the silicon mold. Yao et al.[6] used high internal phase emulsion polymerization in combination with block copolymer chemistry to produce porous polymer with pore size about 5.7 μm. However, the integration of the porous polymer onto the microchannels remains a challenge. Nordborg et al.[7] prepared polymethacrylate-based monoliths by thermal-initiated polymerization; the pore size could be as large as 3.8 μm, but the reaction time was as long as about 24 h. Altun et al.[8] and Yu et al.[9] reported an approach to prepare porous polymer by photoinitiated free radical polymerization. Photoinitiated polymerization usually uses photosensitive initiator to start the polymerization; the reaction can be conducted at room temperature and can be completed in short of time. Molecular weight of polymers formed is expected to be narrow because it does not experience temperature ramping and cooling process as occurred in thermal-initiated polymerization. Another important feature for photoinitiated polymerization is that the porous structure can be *in situ* generated and integrated in the desired position of channels in microfuidic devices by using a mask.

In this article, porous polymers using acrylate monomers are prepared by photoinitiated polymerization. The porous properties such as porosity, pore size, and pore size distribution are systematically

Correspondence to: S. Yu (szyu@SIMTech.a-star.edu.sg).

studied as a function of the composition of the starting solution as well as the synthesis parameters.

EXPERIMENTAL

Materials

The starting solution included monomers, initiator, and porogen. Two types of acrylic monomers were used, one was butyl methacrylate (BMA), and another one was ethylene glycol dimethacrylate (EDMA). The initiator used was UV sensitive initiator, 2-dimethoxy-2-phenylacetophenone. The porogen used was methanol; it also acted as a solvent to dissolve all the reagents in the solution. All the materials were purchased from Sigma Aldrich.

Preparation of porous polymer

The monomers and initiator were dissolved in the porogenic solvent of methanol. The fractions of initiator, monomers, and porogen were varied to study their effects on porous properties. The optimized concentrations of the reagents were: initiator of 3–5% of weight of monomers, BMA/EDMA weight ratio of 50/50 to 30/70, and methanol weight fraction of 0–65%. The starting solution was placed into a UV reactor (Techno-Digm, UV flood UVF 400). The UV chamber equipped with UV lamp of 365 nm, and the UV intensity at different distance to UV lamp was evaluated by an irradiance meter, UV cure plus II (EIT Instrument Markets). The time for polymerization was fixed for 15 min at room temperature regardless the distance from UV lamp to the solution.

Characterization of the porous polymer

The morphology of the porous polymer was observed by several scanning electron microscopes (SEM): extended pressure SEM (Carl Zeiss EVO 50), conventional SEM (Carl Zeiss Stereo Scan S360), and field emission SEM (FESEM, Jeol JSM 6340F). For all the SEMs, the micrographs of the porous polymers were taken with different magnifications. Additionally, it was found that there was no difference in morphology when the samples were observed in cross-section or top view. The open porosity, pore size, and pore size distribution were determined using mercury intrusion porosimetry of AutoPore IV 9500 (Micromeritics Instrument Corporation).

RESULTS AND DISCUSSION

Pore formation mechanism

Two types of monomers were used here, one was BMA with one vinyl group, and another one was EDMA with two vinyl groups. Thus, EDMA divinyl monomer also acts as crosslinking agent in the reaction. In the early stage of the reaction, polymerization conducts homogeneously in the solution as the polymers formed have low molecular weight and can dissolve in the methanol. With the reaction, the polymers formed finally become insoluble in methanol due to the chain propagation and crosslinking, and precipitate from the solution, phase separation occurs at this moment. The precipitated polymers form seed nuclei, the further polymerization and crosslinking reaction of the monomers will conduct in solution and on the nuclei at the same time. Gradually, all polymers formed precipitate from the solution and the nuclei grow in size and form particles, thus the porous polymer matrix forms. The removal of the porogenic solvent between the particle clusters results in the formation of porous structure.

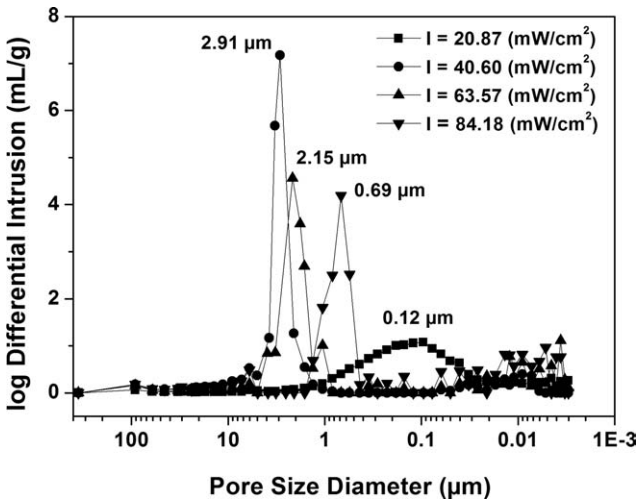

Figure 1 Log differential pore size distribution profile as a function of UV intensity (BMA/EDMA = 50/50, initiator fraction = 3%, porogen = 55%).

It is expected that porous polymers with bigger pores will be formed with earlier phase separation. Any factors affecting the phase separation will affect the porous properties of the polymers. These factors include polymerization rate and crosslinking rate. Therefore, the processing parameters such as UV intensity and composition of the starting solution such as initiator concentration, BMA/EDMA ratio, and methanol fraction can be used to control the porous structure of the polymers.

Effect of UV intensity

Four different UV intensities were used in the synthesis. Figure 1 shows the pore size obtained from mercury intrusion as a function of UV intensity, the pore sizes at the maximum of the pore size distribution curves are also labeled in the Figure. Table I shows the median pore size and porosity obtained

TABLE I
Porous Properties of Porous Polymers with Different UV Intensities

UV intensity (mW/cm^2)	Porosity (%)	Median pore size (μm)
20.87	55.25	0.14
40.60	53.09	2.98
63.57	53.90	2.23
84.18	54.46	0.42

(BMA/EDMA = 50/50, initiator fraction = 3%, and porogen fraction = 55%).

from the porosimetry. It is noted that the porosity listed was corrected with a corresponding blank run. The blank run uses the sample with the same composition of the solution but with no addition of porogenic methanol. The blank correction is necessary due to the compressibility of the samples.[10]

The light intensity is a key factor in photoinitiated polymerization as it controls directly the generation of radicals, a more complete polymerization is achieved upon intense illumination.[11] For the porous polymer synthesized at very low UV intensity of 20.87 mW/cm^2, the median pore size is about 0.14 μm, which is the lowest one among the four samples. Under this low light intensity, the conversion of the monomer to crosslinked polymer might be low, the molecular chains of macromolecules formed are also relatively short, and therefore, the pore dimensions are also small. The low conversion of this polymer can be confirmed by SEM micrographs. Figure 2 shows the SEM images for the porous polymer with different UV intensities. The morphology of the porous polymer formed with light intensity of 20.87 mW/cm^2 is very different from the one formed at 63.57 mW/cm^2, it does not yet form obvious granular structure, suggesting low molecular weight.

With the further increase of UV intensity from 40.60 to 84.18 mW/cm^2, it can be seen that the porosity of porous polymers is almost unchanged, but the median pore size decreases from 2.98 to 0.42 μm due to the increased initiation rate. Under the UV intensity of 63.57 mW/cm^2, the median pore size is about 2.23 μm, which can be widely used in microfluidic filtration applications. This UV intensity is used in the following sections to study the effect of initiator fraction, BMA/EDMA fraction, and methanol concentration.

Besides the effect of UV intensity on the conversion of polymerization and initiation rate, the temperature in the UV chamber is also influenced by the UV intensity. It is measured that the UV chamber is about 38, 47, 63, and 72°C, respectively, at UV intensity of 20.87, 40.60, 63.57, and 84.18 mW/cm^2. The temperature is higher at higher UV intensity. As higher temperatures also lead to increased initiation and polymerization rate, this effect also results in porous polymers with smaller pores.

When we compare the pore size obtained from mercury penetration and from SEM, it can be seen that the pore size obtained from SEM is much larger than that obtained from mercury intrusion. Pore size obtained from mercury porosimetry, actually, is calculated from the corresponding pressure, which is required to force the mercury entering into the pores during the test, using Washburn's equation assuming of cylindrical pore model.[12] However, pores with ideal circular cross-section or any other regular geometry are rarely encountered in porous materials. So, the pore size measured with porosimetry is not the actual inner size of a pore but the largest entrance or throat toward a pore. On the contrary, SEM observes the morphology of the porous sample; it reveals the cavity size of a pore. Therefore, it is obvious that the

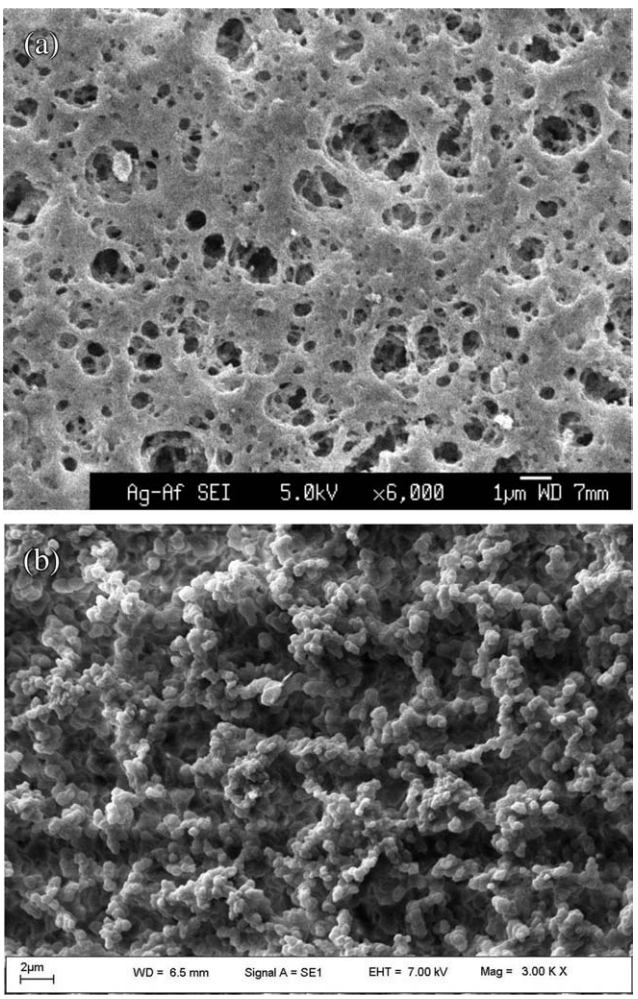

Figure 2 SEM micrographs of porous polymers at different UV intensities (a) UV intensity = 20.87 mW/cm^2, the magnification of the images is 6000×, and (b) UV intensity = 63.57 mW/cm^2, the magnification of the images is 3000×. (BMA/EDMA = 50/50, initiator fraction = 3%, and porogen fraction = 55%).

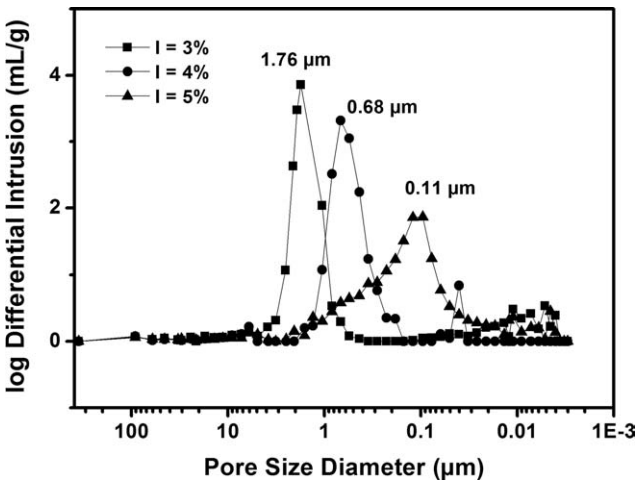

Figure 3 Log differential pore size distribution profile as a function of initiator concentration (BMA/EDMA = 40/60, UV intensity = 63.57 mW/cm^2, and porogen fraction = 55%).

pore size determined by mercury porosimetry is always smaller than the corresponding pore size determined from microscopes.

Effect of initiator concentration

Figure 3 and Table II show the effect of initiator concentration on the porous structure of the porous polymers. Very similar to UV intensity effect, with increasing of initiator concentration, the porosity is almost not affected, but the pore size decreases. With initiator concentration of 5%, the median pore diameter obtained from mercury measurement is only about 0.16 μm, and the pore size distribution is also broad when compared with those with initiator concentration of 3 and 4%. These results are not unexpected. Initiation is a process to create free radicals necessary for chain propagation, with the higher concentration of initiator, more monomers are activated to form monomer radicals under the same UV intensity, and more numbers of nuclei are formed, therefore, the polymerization rate is higher. These nuclei compete monomers for growth, as a result, the size of nuclei formed is smaller, and the pores formed between the particle clusters are also smaller. Additionally, the increase in the photoinitiator concentration also results in the increase in the recombination reaction of the radicals, which also leads to the formation of small nuclei. Figure 4 is the SEM micrographs, the clusters formed with 5% of initiator is obviously smaller than those with 4 and 3% of initiator.

TABLE II
Porous Properties of Porous Polymers with Different Photoinitiator Concentrations

Initiator (%)	Porosity (%)	Median pore size (μm)
3	54.00	1.6
4	51.09	0.67
5	53.03	0.16

BMA/EDMA = 40/60, UV intensity = 63.57 mW/cm^2, and porogen fraction = 55%.

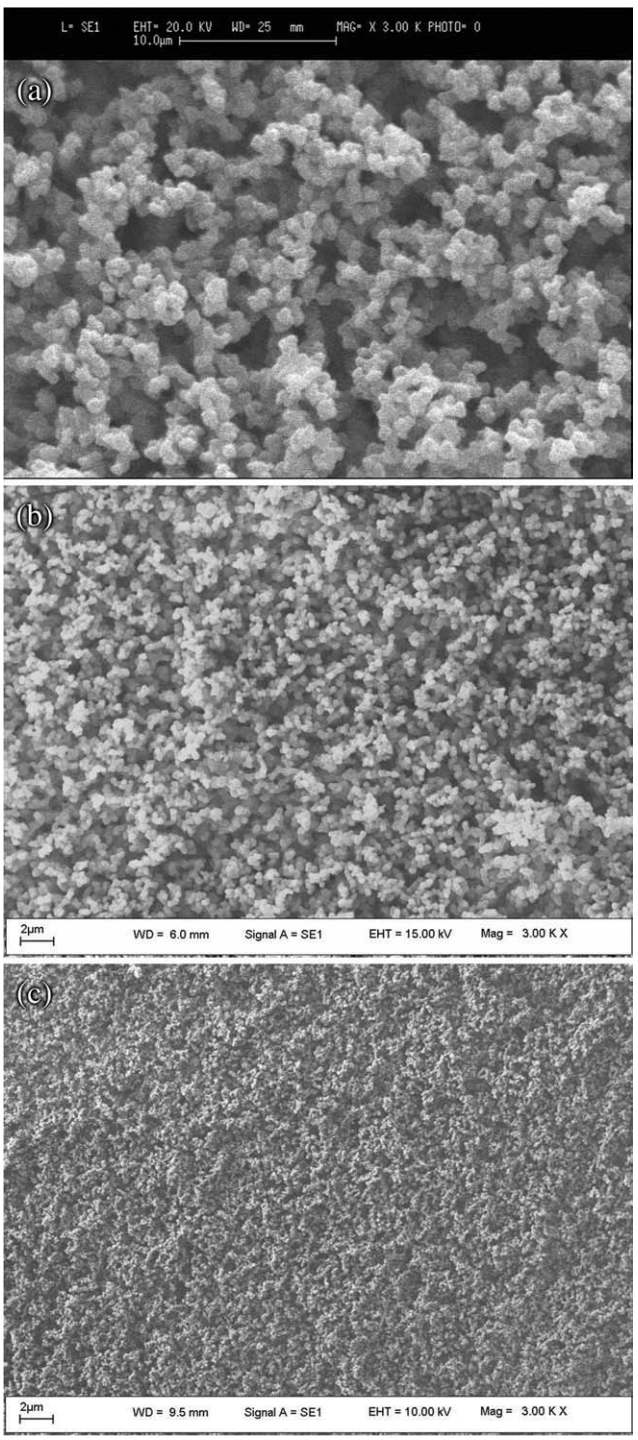

Figure 4 SEM micrographs of porous polymers with different initiator concentrations (a) initiator fraction = 3%, (b) initiator fraction = 4%, and (c) initiator fraction = 5%, the magnification of the images is 3000×. (BMA/EDMA = 40/60, UV intensity = 63.57 mW/cm^2, and porogen fraction = 55%).

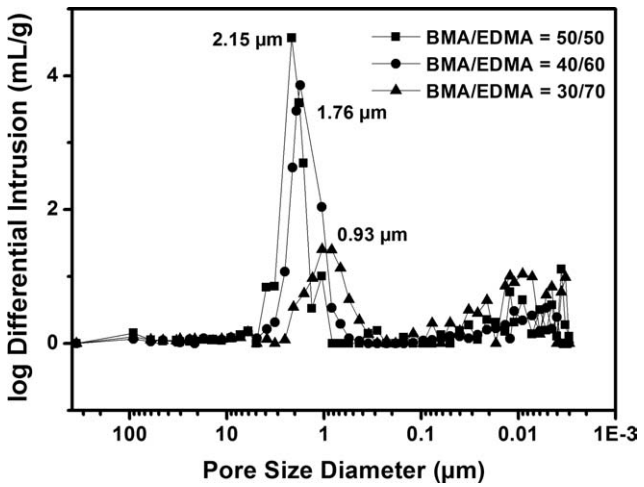

Figure 5 Log differential pore size distribution profile as a function of BMA/EDMA concentrations (initiator = 3%, UV intensity = 63.57 mW/cm^2, and porogen = 55%).

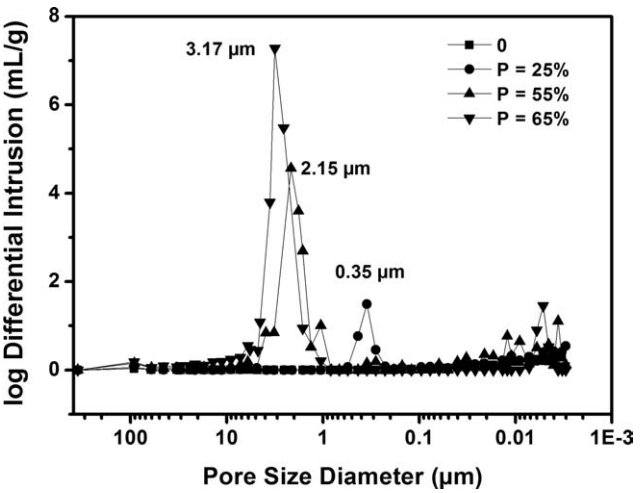

Figure 6 log differential pore size distribution profile as a function of porogen fractions (BMA/EDMA=50/50, initiator = 3%, and UV intensity = 63.57 mW/cm^2).

Effect of crosslink agent concentration

Changing of monovinyl monomer and divinyl monomer ratio is another effective approach to tailor the porous properties. When the BMA and EDMA monomer ratio is high such as 70/30 and 60/40, the samples are still either watery or sticky after exposing to UV light for 15 min, indicating that the polymers are not able to generate under these conditions. When the percentage of crosslink agent is high enough to form solid samples, it is found that the pore size decreases with the increasing concentration of the crosslink agent, whereas the porosity is almost unchanged. Figure 5 and Table III show the properties of the porous polymers as a function of BMA/EDMA ratio. EDMA is a divinyl monomer; more monomer radicals will be generated when the fraction of EDMA is increased. Therefore, similar to the effect of initiator concentration, higher EDMA fraction will result in the formation of porous polymers with smaller pores. On the other side, EDMA also acts as crosslinking agent in the reaction, it is easy to understand that denser structure will be formed with higher crosslinking agent. The effect of crosslink agent on the pore size obtained here is similar to that observed by Santora et al.[13] who developed porous polymer from ethylene dimethacrylate/methyl methacrylate monomers using bulk polymerization technique.

Effect of porogen concentration

The porogenic solvent has a significant effect on the porous structure. Figure 6 and Table IV show the effect of methanol fraction on the porosity and pore size of the polymers. With no addition of porogenic methanol, there is no pores observed in SEM, and the porosity obtained from mercury intrusion is regarded as zero (equivalent to blank run). With increasing fraction of methanol, both pore size and porosity of the porous polymers increase. This is understandable as the methanol occupies more spaces at higher fraction, thus, higher porosity and larger pores leave behind after it is removed. However, if the methanol fraction is increased to 75% and beyond, no polymers can be formed. The monomers are separated by the large amount of solvent, and the propagation of the molecular chains is

TABLE III
Porous Properties of Porous Polymers with Different BMA/EDMA Ratios

BMA/EDMA	Porosity (%)	Median pore size (μm)
50/50	53.90	2.23
40/60	51.09	1.60
30/70	55.01	1.02

Initiator fraction = 3%, UV intensity = 63.57 mW/cm^2, and porogen fraction = 55%.

TABLE IV
Porous Properties of Porous Polymers with Different Porogen Fraction

Porogen concentration (%)	Porosity (%)	Median pore size (μm)
0	0	–
25	24.23	0.27
55	53.90	2.23
65	61.05	2.97

(BMA/EDMA = 50/50, UV intensity = 63.57 mW/cm^2, and initiator fraction = 3%).

disturbed. Actually, methanol is a poor solvent to monomers of BMA and EDMA as their solubility parameters are very different, which leads to early phase separation, this, together with the effect of porogen type, will be discussed in detail in another publication.

CONCLUSIONS

Porous polymers with controlled porous properties have been successfully produced by photoinitiated free radical polymerization. Porosity of the porous polymers is mainly porogen concentration dependent. Pore size of the porous polymers is greatly affected by UV intensity, fraction of initiator, fraction of crosslink agent, and porogen concentration. Higher fraction of porogenic methanol will result in porous polymers with higher porosity and larger pore size; higher fraction of initiator, EDMA crosslinking as well as higher UV intensity usually lead to the formation of polymers with smaller pore size.

References

1. Sederel, W. L.; DeJong, G. J. J. Appl Polym Sci 1973, 17, 2835.
2. Meyer, U.; Svec, F.; Fréchet, J. M. J. Macromolecules 2000, 33, 7769.
3. Chang, C.; Yang, C.; Chuang, Y.; Khoo, H.; Tseng, F. Nanotechnology 2008, 19, 365301.
4. Akthuakul, A.; Salinara, R. F.; Mayes, A. M. Macromolecules, 2004, 37, 7663.
5. Jong de, J.; Ankoné, B.; Lammertink, R. G. H.; Wessling, M. Lab Chip 2005, 5, 1240.
6. Yao, C.; Qi, L.; Jia, H.; Xin, P.; Yang, G.; Chen, Y. J. Mater Chem 2009, 19, 767.
7. Nordborg, A.; Svec, F.; Fréchet J. M. J.; Irgum, K. J Sep Sci 2005, 28, 2401.
8. Altun, Z.; Hjelmström, A.; Abdel-Rehim, M.; Blomberg, L. G. J Sep Sci 2007, 30, 1964.
9. Yu, C.; Svec, F.; Fréchet, J. M. J. Electrophoresis 2000, 21, 120.
10. Schüth, F.; Sing, K. S. W.; Weitkamp, J., Eds. Handbook of Porous Solids, Vol. 1; Wiley-VCH: Weinheim, Germany, 2002.
11. Decker, C.; Decker, D.; Morel, F. In Photopolymerization; Scranton, A. C.; Bowman, C. N.; Peiffer, R. W., Eds.; ACS Symposium Series 673: Washinton DC, 1997; p 63.
12. Washburn, E. W. Phys Rev 1921, 17, 273.
13. Santora, B. P.; Gagné, M. R.; Moloy, K. G.; Radu, N. S. Macromolecules 2001, 34, 658.